

Spectrally selective heating of nanosized particles by surface plasmon resonance

E.A. Hawes^{a,*}, J.T. Hastings^b, C. Crofcheck^a, M.P. Mengüç^c

^aUniversity of Kentucky, 128 C.E. Barnhart Building, Lexington, KY 40503, USA

^bUniversity of Kentucky, 453 Anderson Hall, Lexington, KY 40503, USA

^cUniversity of Kentucky, 269 Ralph G. Anderson Building, Lexington, KY 40503, USA

Received 10 July 2006; accepted 28 July 2006

Abstract

We present a series of computer simulations of 10 nm particles optically excited at their surface plasmon resonance. These simulations are focused on gold and silver nanocylinders, resting on either on a thin metallic film or on a glass surface. The results indicate that excitation is highly dependent on both the material and the proximity of other particles. These findings suggest that manipulation and assembly of nanoparticles is feasible. This study also underlines the importance of computational radiation transfer research for the successful implementation of novel nanomachining processes.

© 2006 Elsevier Ltd. All rights reserved.

1. Introduction

Understanding and manipulating nanosized particles is an active area of nanoscale research. We have recently proposed a novel approach for three-dimensional assembly at the nanoscale, based on selective excitation of metal nanostructures at their surface plasmon resonance (SPR). To further develop this approach we need a better understanding of nanoparticle interactions and the non-bulk properties of nanoscale materials. Numerical analysis of the optical absorption of nanoparticles can lead to a broader understanding of the physics at the nanoscale, may provide a means for extracting non-bulk properties of nanoscale materials *prior* to physical testing, and will provide insight into nanoscale radiative transfer. The results presented form a theoretical framework that will be experimentally verified in later testing.

Directed assembly of nanoscale particles is expected to be a powerful tool, and will be prevalent in the future of advanced engineering applications. The fusing of nanosized metallic particles occurs by melting the surface of the particles. In order to heat the particles selectively and locally, they are excited at their SPR. In order to selectively target nanoparticles, the amount of energy required to melt the surface of the particles and the

*Corresponding author.

E-mail addresses: ederbysh@bae.uky.edu (E.A. Hawes), hastings@enr.uky.edu (J.T. Hastings), ccrofche@bae.uky.edu (C. Crofcheck), menguc@uky.edu (M.P. Mengüç).

Nomenclature

| | |
|------------------|--------------------------|
| C_{abs} | absorption cross section |
| a | particle radius |
| c | speed of light |
| V | domain area |
| J | current density |
| D | electric displacement |
| E | electric field strength |
| t | time |
| L | tensor |
| S | closed boundary |
| H | magnetic field strength |
| B | magnetic flux density |
| P | electric polarization |
| M | magnetic polarization |

Greek symbols

| | |
|---------------|-------------------------|
| ε | dielectric function |
| σ | electrical conductivity |
| ω | angular frequency |
| χ | susceptibility |
| λ | wavelength |
| μ | permeability |

Subscripts

| | |
|---|------------------|
| 0 | vacuum |
| 1 | dielectric |
| r | refractive index |
| m | medium |

Superscript

| | |
|---------------|------------------------------|
| ε | externally generated current |
|---------------|------------------------------|

interaction between the particles must be properly understood. Computational studies allow us to understand the energy needed to fuse the particles and the resolution limits that can be achieved in a practical setting.

The SPR wavelength is determined by a nanostructure's dielectric constant, geometry, and surrounding environment [1]. Gold nanostructures have been extensively studied, and it has been found that spheres smaller than ~ 20 nm behave much like dipoles, with maximum absorption and scattering occurring at wavelengths near 500 nm in air or vacuum. Silver nanostructures exhibit similar behaviour with the various resonances occurring at different wavelengths (about 350 nm) due to the dielectric constant dispersion of silver. These well-known phenomena form the basis for shape and material selectivity in our nanoscale self-assembly system.

Inter-particle spacing, material choice, and SPR all play vital roles in the selective nature of directed assembly. Understanding of these processes will establish the theoretical resolution of the assembly technique, and will provide insight into optimum conditions for localized melting and fusing. Direct solutions for Maxwell's equations are essential to fully understand this phenomenon.

With the calculation of the SPR particular to a metal, one can use the differences in peak resonance for selectivity. For gold, copper, and silver nanoparticles, whose resonance frequencies occur in the near UV and visible spectral regions, the resonance can be used to excite the particles [2,3]. This phenomenon suggests that particles can be excited selectively: if one had gold and silver on the same surface, and an incident light source at 500 nm, only the gold will strongly absorb the light. Additionally, resonance wavelength varies with particle size. As particles increase in size toward 100 nm diameters their resonances shift toward the red portion of the spectrum. Thus, one can control the type of particle (gold, silver, copper and other metals in the non-visible spectrum) and the size of particle that experiences resonance. This control allows for precise patterning techniques in terms of size and material. The success of this will result in an extremely powerful tool for nanoscale manufacturing.

1.1. Radiation at the nanoscale and surface plasmons

Thermal properties of gold particles with diameters smaller than 10 nm are widely divergent from bulk properties. Current models, those of Buffat and Borel [4], Semchenko [5], Pawlow [6], and Kofman [7,8], predict a sharp reduction in melting temperature beginning at ~ 10 nm diameter and decreasing rapidly below ~ 5 nm diameter. As the size of a gold particle decreases from 10 to 5 nm, the surface melting point has been experimentally observed to decrease from 900 to 450 °C, and theoretically predicted to decrease from 620 to 350 °C [9]. Less experimental evidence is available for silver nanoparticle melting, but theoretical studies indicate that silver particles should melt at temperatures significantly less than their bulk melting temperature and that surface pre-melting should also depend on the particle radius [10,11].

The linear optical properties, including SPR, of small metal spheres was explained theoretically by Lorenz in 1891 and Mie [12] in 1908. The Lorenz–Mie theory helps to explain the mechanism of scattering by small particles as well as nanoparticle excitation. Mie solved Maxwell's equations analytically for the interaction of an electromagnetic (EM) field with a small sphere [12]. The calculations provide the absorption, extinction, and scattering characteristics of particles as a function of particle radius, wavelength of the incident radiation, and the relative index of refraction of particle. In the Rayleigh regime [2], the Lorenz–Mie calculations yield a resonance wavelength that is independent of particle size. The specific resonance wavelength is determined by the extinction cross section, which gives the radiant flux scattered and absorbed by the particle and the extinction efficiency [13].

Using the dipole approximation, the absorption cross section, C_{abs} , of nanoparticles can be calculated [14]:

$$C_{\text{abs}} = \frac{8\pi^2 a^3 \sqrt{\epsilon_1}}{\lambda} \text{Im} \left(\frac{\epsilon_1 - \epsilon_m}{\epsilon_1 + 2\epsilon_m} \right). \quad (1)$$

Although the dipole approximation results in resonance condition that is independent of size, the resonance wavelength actually varies strongly with size [15]. For very small particles (< 2 nm) the bulk dielectric constant can no longer be used to model the particle, and the plasmon resonance becomes less distinct [16]. The reason for this deviation in behaviour from larger particles has been suggested to be a result of a smaller mean free path for conduction electrons, resulting in an enhancement of electron–surface scattering [17–19]. If one wishes to use the Lorenz–Mie theory to calculate absorption and scattering for such small particles, the dielectric constant must be modified based on the particle size [17–19]. Mie theory is applicable to single particles that are assumed to be non-interacting and are separated by a distance larger than the particle radius [14]. Within this inter-particle distance, the particles affect one another. Inter-particle dynamics influence the spread of energy throughout the system. Mie's work serves as a starting point. The computation simulations, which agree with Mie theory when the particles are separated by the inter-particle distance, provide a theoretical template for interacting particle behaviour. Understanding of these inter-particle dynamics can be achieved by mapping the distribution of electric field and intensity around the particles, excited by surface plasmons, as they change proximity to one another.

The Lorenz–Mie theory fails to explain the resonance conditions when particles aggregate and to explain why bulk dielectric constants no longer apply when particles become small (somewhere between 5 and 20 nm in diameter). Several groups have proposed useful extensions to Mie theory using a size-dependent dielectric constant to account for quantum size effects and surface scattering [18]. We have recently extended the

Lorenz–Mie theory using numerical techniques that account for particle–particle and particle–surface interactions [20–22]. These techniques calculate the scattering by the particles, and are currently being modified to include the absorption by aggregated particles. These theories form the foundation for estimating the optimal illumination wavelengths for various particles in our nanoassembly system.

As with the Lorenz–Mie theory calculations, radiation transfer at the nanoscale has limited analytical solutions. Available studies are typically numerical, for simple geometries [23], and use EM approaches [24]. In conjunction with the numerical program developed by Venkata [22], the results of this study can be used to develop a broader picture of radiation at the nanoscale. Our combined results provide the scattering and absorption of a variety of small particles on a surface, including single and aggregated particles with various materials. Additionally, these hybrid calculations encompass both the near- and far-field results.

2. Methods and materials

To examine the interactions between the particles experiencing SPR, particles of 10 nm in diameter were considered. The particles were examined in two dimensions, and as such are considered infinite cylinders. The change in resistive heating and energy was extracted as the particles change proximity to one another. Three situations were simulated: (1) particles on a glass surface illuminated using total-internal-reflection (TIR) [25], (2) particles on a thin silver film illuminated through the silver, and (3) particles on a thin gold surface illuminated from below the gold layer.

The simulations were carried out to observe the resonance conditions on glass and on a thin silver film. The change in absorption in a gold and silver particle as it moves away from another particle of the same material and the change in absorption of a gold and silver particle as they are separated were determined. Each particle tested was 10 nm in diameter, and was simulated from 1 to 10 nm separation distance from another particle. To create surface plasmon excitation, an angled electric field (TIR) at 45° was transmitted through glass and was assumed to be incident upon a thin silver surface (20 nm). This same situation was repeated for particles on a glass surface with no metallic interface. Above the surface sit gold and silver particles in vacuum. The results of these simulations were then compared to current theory and used to determine the energy needed to heat the particles to melt the surface or bulk. This analysis is expected to shed light on the feasibility of selective heating based on particle size.

2.1. Governing equations, boundary conditions and considerations

The primary input parameter used for simulations was the wavelength-dependent index of refraction. The index of refraction accounts for the polarization of the material in response to an electric field [26] and is considered an intrinsic property at the size scale employed. We assume the relative permeability is 1 for all our simulations, because gold is non-magnetic. Maxwell's equations can be solved, using appropriate indices of refraction and geometry, to determine the resistive heating of the material (W/m^3) [26]. The absorption of the particle can be calculated from this information, by a simple energy balance calculation.

The governing equations used in simulations are Maxwell–Ampere's law and Faraday's law, which are well known. These equations describe the time and space of the EM field. For the simulations presented here, we solved the wave equation for the transverse magnetic field, H_z , given by $\nabla \times (\epsilon_r^{-1} \nabla \times H_z) - \mu_r k_0^2 H_z = 0$. The constitutive relations can be used to describe the polarization of the electric field and magnetic field. The polarization of the electric and magnetic field are directly proportional to the field strength, because the materials are linear and isotropic. This proportionality allows one to use the well-known relations: $P = \epsilon_0 \chi_e E$ and $M = \chi_m H$. Combining Maxwell–Farady equations with the constitutive relations, and using the relations $D = \epsilon_0 E + P$, $J = \sigma E$ and $B = \mu_0(H + M)$ yields:

$$D = \epsilon_0(1 + \chi_e)E = \epsilon_0 \epsilon_r E, \quad (2)$$

$$B = \mu_0(1 + \chi_m)H = \mu_0 \mu_r H. \quad (3)$$

Through the equations describing the energy time derivative of the electric and magnetic fields (power), one can relate the properties to the resistive and radiative energy via Poynting's theorem:

$$-\int_V \left(E \frac{\partial D}{\partial t} + H \frac{\partial B}{\partial t} \right) dV = \int_V JE dV + \oint_S (E \times H) n dS. \quad (4)$$

Resistive losses are described by the first term on the right-hand side of the equation and radiative losses are described by the second term on the right-hand side.

The resistive heating is calculated using

$$\frac{1}{2} \text{Re} \{ \sigma EE^* - j\omega ED^* \}. \quad (5)$$

2.1.1. Boundary conditions

Two boundary conditions were applied to the two-dimensional analysis. The boundaries were designed so that one boundary was a source for the incident EM field. The other boundaries, which closed the geometrical system, were programmed to be non-reflective.

The incident EM boundary was a user-defined electric or magnetic field input. These fields were angled in the x - y plane with respect to the z -axis, to achieve the required incident angle. The EM fields were kept constant for each simulation in order to ensure accurate comparative results.

To ensure that the boundaries did not interfere with the wave propagation, the boundaries used were 'perfectly matched layers' (PML). The PML absorbs the incident radiation without producing reflection. As such, the PML is implemented as a material with an anisotropic permittivity and permeability, which matches the adjacent medium.

2.2. Error considerations

The computational studies have used COMSOL© Multiphysics version 3.2 to implement the finite element method and numerically solve Maxwell's equations. Numerical uncertainty is based primarily on the number of mesh elements used and the geometry. The primary factor is the mesh refinement used, which is user-defined. The mesh used had a resolution of 0.01 elements/nm.

To determine the error associated with a particular geometry, an error assessment was made prior to testing. For example, the error for a silver and gold on glass with 5329 degrees of freedom and 2634 elements/ 10^{-12} m^2 gives an extremely high t -value (10^{-8}), which corresponds to COMSOL©'s own error analysis output (3.30512×10^{-8}). The error changes with each geometry: the mesh is adaptive to the individual geometrical considerations, and as such, the number of elements within a mesh vary marginally (and statistically insignificantly) with each simulation. Other studies were conducted to analyse COMSOL©'s accuracy [25,27]. From this research standpoint, COMSOL©'s output was considered accurate if its results matched the results of analytical solutions.

The purpose of the simulations is to look *beyond* what is analytically calculable. Theoretically, the output produces solutions that will be accurate according to Maxwell's equations. With this numerical data, and confirmation by theory and available data, the next step is to test the theory in a laboratory setting. At this point the data provides a theoretical framework for such experiments.

3. Results and discussion

The present study focuses on examining the spatial effect of gold and silver particles and the selective excitation of particles in terms of SPR. The energy required to fuse gold particles was determined theoretically with models discussed above. Below we will discuss a series of simulations for different particle sizes and incident light wavelengths to show the feasibility of the idea.

3.1. Absorption by gold and silver particles on a glass surface

3.1.1. Gold particles on glass

Fig. 1(a) shows the predictions for different size particles; the peak absorption occurs at 490 nm wavelength. At both resonance (250 nm) and peak absorption (490 nm) wavelengths for gold, no significant shift in wavelength is observed for either a single or two particle cases. At wavelengths shorter than 490 nm, the particles experience no significant change in absorption efficiency. However, at wavelengths longer than 490 nm, the decrease in absorption occurs more rapidly for particles at larger separation distances. This change indicates that particles closer to one another suppress absorption at peak resonance, but increase absorption at higher wavelengths. At peak resonance, particles modelled between 1 and 10 nm separation distance experience an overall absorption difference of 8%.

Gold particles 1 nm apart have virtually the same absorption as those 5 nm apart. Particles that are 2, 3, and 4 nm apart share the same absorption efficiency magnitude, which is slightly lower than 1 and 5 nm (by about 3%). Above a 5 nm separation distance, the particles increase in absorption corresponding to an increase in distance. There is no secondary peak for gold on glass.

3.1.2. Silver particles on glass

Silver particles experience no substantial shift in peak absorption at separation distances from 1 to 10 nm. Peak absorption occurs at the cylinder SPR near 340 nm. An increase in separation distance between particles directly parallels an increase in absorption. The total change in absorption efficiency over distances between 1 and 10 nm is small (3–4.5%), which indicates limited spatial selectivity between two silver particles. Additionally, as separation distance increases, the change in absorption becomes smaller.

At wavelengths longer than 340 nm, particles at larger separation distances show a more rapid decrease in absorption efficiency than when particles are closer together. For this longer wavelength range, absorption efficiency tends to merge to a single line, as shown in Fig. 1(b). Interestingly, at wavelengths longer than 340 nm, there is an inversion between separation distance and absorption efficiency: the 1 nm separation distance yields larger absorption efficiency than larger separation distances. For particles 1 nm in separation, there is a secondary absorption peak at 380 nm. The difference at 380 nm between a separation distance of 1 and 10 nm is 33%.

3.1.3. Gold and silver on glass

In the presence of a gold particle, the silver absorption peak shifts from 340 to 350 nm, and is 10 times the magnitude of that gold particle. Gold also experiences a change in absorption peaks. In the presence of a silver particle, a gold particle experiences two absorption peaks, at 340 and 490 nm. A silver particle does not affect the magnitude of absorption for a gold particle. The presence of a gold particle has a more dramatic effect on a silver particle, decreasing the magnitude of absorption by a factor of 10. These results are depicted in Fig. 3(a).

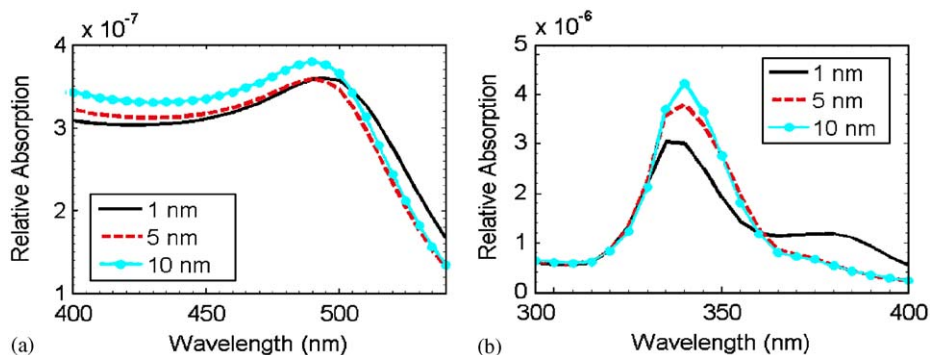


Fig. 1. Absorption (C_{abs}) of gold (a) and silver (b) particles on glass versus wavelength. The absorption is shown as particle separation increases from 1 to 10 nm.

3.2. Absorption by gold and silver particles on a silver surface

3.2.1. Gold and gold on silver

The 10 nm gold particles experience peak absorption at 465 nm on a 20 nm thin silver film. This peak does not shift as a function of separation distance between two same-size particles (see Fig. 2(a)). As particles separate, the absorption shows no significant magnitude change (less than 1%). Gold particles are almost 40 times less responsive on silver than on a glass substrate.

3.2.2. Silver and silver on silver

As they separate in distance, there is no shift of resonance peak for silver particles on a thin silver substrate. They experience a peak resonance at 490 nm and a secondary peak at 280 nm, as seen in Fig. 3(b). Smaller separation distance yields slightly lower absorption (about 3.5%). Silver is almost 50 times less responsive on a silver film compared to glass substrate.

3.2.3. Gold and silver on silver

On a silver substrate and in the presence of a silver particle, gold has an absorption peak at 460 nm. Likewise, the peak resonance for a silver particle on a silver substrate changes in the presence of gold to 480 nm. These results are depicted in Fig. 3(b). The absorption decreases with decreasing distance between particles. Gold particles show about 30% increase in absorption range if they are near a silver particle rather

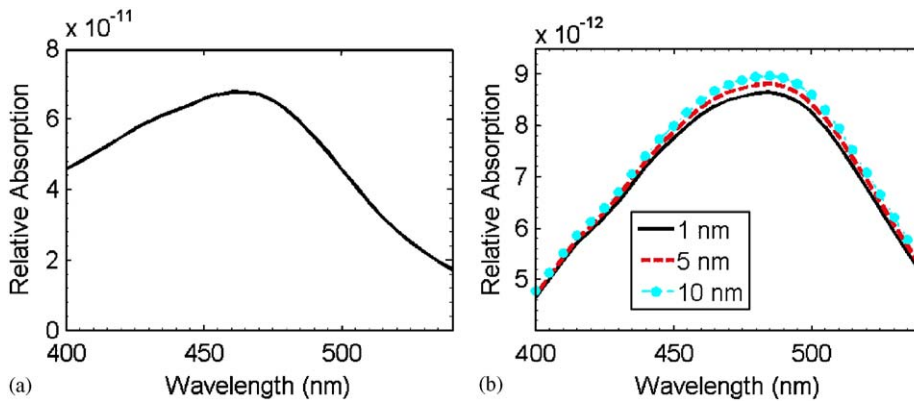


Fig. 2. Absorption (C_{abs}) of gold (a) and silver (b) particles on silver substrate versus wavelength. The absorption is shown as particle separation increases from 1 to 10 nm.

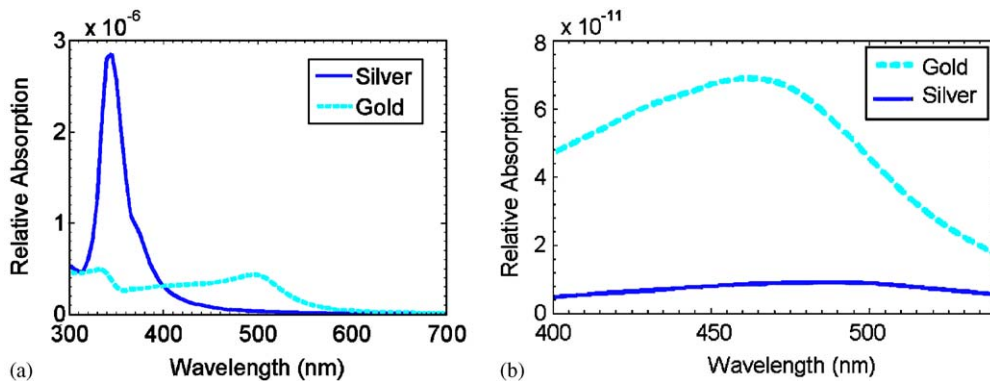


Fig. 3. Absorption (C_{abs}) of gold and silver particles on glass (a) and on silver substrate (b) versus wavelength.

than a gold particle. Silver experiences a 25% increase in absorption. Gold's absorption is about 10 times larger than that of silver.

3.3. General remarks

The absorption peak results are in good agreement with the available data. For silver particles on glass, which have an absorption peak at 340 nm, our findings concur with the results from Kottman and Martin [23] and Zou et al. [28]. Kottman and Martin determined the absorption for 20–50 nm silver nanowires, which are approximated in our simulations as infinite cylinders. Equally, the gold particles on a glass surface are in good agreement with experimental results [29]. The results are also in agreement with the literature for silver particles on a silver surface. The data from Zou et al. [28] indicates that the red-shifting that occurs with introduction of a second silver particle, similar to what we have seen. The confirmation of our predictions with the published results lends credence to our simulations, the examination of silver and gold, and gold on a thin silver film. Our results form what we believe to be an accurate theoretical framework for experimental design.

4. Summary

We presented a series of computer simulations of 10 nm particles optically excited at their SPR. These simulations, carried out with COMSOL[®] Multiphysics code, are focused on gold and silver nanocylinders, resting either on a thin metallic film or on a glass surface. Simulations indicated a significant interaction between particles at a distance smaller than the dominant diameter. The results demonstrated that absorption depends significantly on both particle separation and substrate material. With precise conditions needed to raise the energy of the particle to its melting point, the development of a highly selective fusing process at the nanoscale does appear possible. This study also underlines the importance of computational radiation transfer research based on the solution of Maxwell equations for the successful implementation of novel nanomachining processes.

Acknowledgements

We would like to thank the University of Kentucky Honors Program for the support E.A.H received during the course of this study.

References

- [1] Raether H. Surface plasmons on smooth and rough surfaces and on gratings. New York: Springer; 1988.
- [2] Link S, El-Sayed M. Optical properties and ultrafast dynamics of metallic nanocrystals. *Annu Rev Phys Chem* 2003;54:331–66.
- [3] Hartland GV, Hu M. Softening of the symmetric breathing mode in gold particles by laser-induced heating. *J Phys Chem B* 2003;107:7472–8.
- [4] Buffat P, Borel J-P. Size effect of the melting temperature of gold particles. *Phys Rev A* 1976;13(6).
- [5] Semchenko VK. Surface phenomena in metals and alloys. Oxford: Pergamon Press; 1981.
- [6] Pawlow P. *Z Phys Chem* 1909;65:545.
- [7] Kofman R, Cheyssac P, Aouaj A, Lereah Y, Deutscher G, Ben-David T, et al. Surface melting enhanced by curvature effects. *Surf Sci* 1994;303:231.
- [8] Lereah Y, Kofman R, Penisson JM, Deutscher G, Cheyssac P, David TB, et al. Time resolved electron microscopy studies of the structures of nanoparticles and their melting. *Philos Mag B* 2001;81(11):1801–19.
- [9] Cortie M. The Weird world of nanoscale gold, Vol. 27. *Gold Bulletin*; 2004.
- [10] Mottet C, Goniakowski J, Baletto F, Ferrando R, Treglia G. Modeling free and supported metallic nanoclusters: structure and dynamics. *Phase Transitions* 2004;77:101–13.
- [11] Zhao S, Wang S, Ye H. Size-dependent melting properties of free silver nanoclusters. *J Phys Soc Japan* 2001;70:2953–7.
- [12] Mie G. Articles on the optical characteristics of turbid tubes, especially colloidal metal solutions. *Ann Phys* 1908;25:377–445.
- [13] Chylek P, Zhan J. Interference structure of the Mie extinction cross section. *J Opt Soc Am A* 1989;6:1846.
- [14] Bohren CF, Huffman DR. Absorption and scattering of light by small particles. New York: Wiley; 1983.
- [15] Kreibitz U, Vollmer M. Optical properties of metal clusters. Berlin: Springer; 1995.
- [16] Alvarez MM, Khoury JT, Shafiqullin MN, Vezmer I, Whetten RL. Optical absorption spectra of nanocrystal gold molecules. *J Phys Chem B* 1997;101:3706.

- [17] Kreibig U, von Fragstein C. Limitation of electron mean free path in small silver particles. *Z Phys* 1969;224:307.
- [18] Kreibig U, Genzel L. Optical absorption of small metallic particles. *Surf Sci* 1985;156:678.
- [19] Kreibig U. Kramers Kronig analysis of optical properties of small silver particles. *Z Phys* 1970;234:307.
- [20] Videen GM, Aslan MM, Mengüç MP. Characterization of metallic nanoparticles via surface wave scattering: A. theoretical framework. *JQSRT* 2005;93:195–206.
- [21] Aslan MM, Mengüç MP, Videen G. Characterization of metallic nanoparticles via surface wave scattering: B. physical concept and numerical experiments. *JQSRT* 2005;93:207–17.
- [22] Venkata PG, Aslan MM, Mengüç MP, Videen G. The surface plasmon scattering patterns from gold nano-particles and agglomerates. Orlando, FL: ASME-IMECE; 2005 [to be submitted to *ASME J Heat Transfer*].
- [23] Kottman JP, Martin OJF. Plasmon resonances of silver nanowires with a nonregular cross section. *Phys Rev B* 2001;64.
- [24] Mulet JP, Joulain K, Carminati R, Greffet J-J. Nanoscale radiative heat transfer between a small particle and a plane surface. *Appl Phys Lett* 2001;78(19):2931–3.
- [25] Ford GW, Weber WH. Electromagnetic interactions of molecules with metal surfaces. *Phys Rep* 1984;113(4):197–287.
- [26] Feibelman PJ. Surface electromagnetic fields. *Prog Surf Sci* 1982;12:287–408.
- [27] Hanke M. Benchmarking FEMLAB 3.0a. Report no. 2004:01, Parallel and Scientific Computing Institute; 2004.
- [28] Zou S, Janel N, Schatz G. Silver nanoparticle array structures that produce remarkably narrow plasmons lineshapes. *J Chem Phys* 2004;120(23):10871–5.
- [29] Kim B, Tripp S, Wei A. Tuning the optical properties of large gold nanoparticle arrays. *Materials Research Society symposium proceedings*; 2001; 676.